On the use of the Boussinesq equation for interpreting recession hydrographs from sloping aquifers

David E. Rupp[1,2] and John S. Selker[1]

Received 2 April 2006; revised 13 July 2006; accepted 1 August 2006; published 28 December 2006.

[1] The method of recession analysis proposed by Brutsaert and Nieber (1977) remains one of the few analytical tools for estimating aquifer hydraulic parameters at the field scale and beyond. In the method, the recession hydrograph is examined as $-dQ/dt = f(Q)$, where Q is aquifer discharge and f is an arbitrary function. The observed function f is parameterized through analytical solutions to the one-dimensional Boussinesq equation for unconfined flow in a homogeneous and horizontal aquifer. While attractive in its simplicity, as originally presented it is not applicable to settings where slope is an important driver of flow, or where hydraulic parameters vary greatly with depth. We compare analytical solutions to the linearized one-dimensional Boussinesq equation for a sloping aquifer to numerical solutions of the full nonlinear equation. The behavior of the nonlinear Boussinesq equation is also assessed when the aquifer is heterogeneous wherein the lateral saturated hydraulic conductivity k varies as a power law with height z above the impermeable layer ($k \sim z^n$, n constant ≥ 0). All of the analytical solutions differ in key aspects from the nonlinear solution when plotted as $-dQ/dt = f(Q)$ and thus are inappropriate for a Brutsaert and Nieber-type analysis. However, new analytical solutions for a sloping aquifer are derived "empirically" from the numerical simulations that are applicable during the late period of recession when the recession curve converges to $-dQ/dt = aQ^b$, where $b = (2n + 1)/(n + 1)$ and a is a function of the dimensions and hydraulic properties of the aquifer.

Citation: Rupp, D. E., and J. S. Selker (2006), On the use of the Boussinesq equation for interpreting recession hydrographs from sloping aquifers, *Water Resour. Res.*, *42*, W12421, doi:10.1029/2006WR005080.

1. Introduction

[2] Recession flow analysis for forecasting drought flows and investigating the groundwater flow regime in basins has over a century-long history (see reviews by *Hall* [1968] and *Tallaksen* [1995]). *Brutsaert and Nieber* [1977] made a landmark contribution when they proposed plotting the observed recession slope of the drought flow hydrograph, or dQ/dt, against the discharge Q, such that

$$-\frac{dQ}{dt} = f(Q), \tag{1}$$

where f denotes an arbitrary function, and compared observations with analytical solutions to the Boussinesq equation for one-dimensional (1-D) flow in a rectangular horizontal aquifer. This method of analysis, referred to hereinafter as "recession slope analysis," has been used widely since to determine aquifer parameters [*Brutsaert and Nieber*, 1977; *Vogel and Kroll*, 1992; *Troch et al.*, 1993; *Brutsaert and Lopez*, 1998; *Szilagyi et al.*, 1998; *Eng and Brutsaert*, 1999; *Parlange et al.*, 2001; *Mendoza et al.*, 2003; *Rupp et al.*, 2004; *Malvicini et al.*, 2005], for base flow separation [*Szilagyi and Parlange*, 1998], and as an aid toward understanding the processes controlling groundwater discharge to streams [*Tague and Grant*, 2004]. Recession curves plotted as $-dQ/dt$ versus Q, or similarly in log-log space, will be referred to as "recession slope curves" hereinafter.

[3] The primary function of presenting the recession curve as $-dQ/dt$ versus Q is the elimination of time as the dependent variable, thus making it unnecessary to determine the precise beginning of the recession event, t_0 [*Brutsaert and Nieber*, 1977]. The ambiguity of t_0 in real discharge data leads to uncertainty in the parameterization of groundwater outflow functions.

[4] However, what has certainly made this method of analysis alluring is that three well-known analytical solutions to the Boussinesq equation for an unconfined horizontal aquifer (two exact solutions [*Boussinesq*, 1904; *Polubarinova-Kochina*, 1962] and one an approximation by linearization [*Boussinesq*, 1903]) can be expressed in the form

$$-\frac{dQ}{dt} = aQ^b, \tag{2}$$

where b is a constant and a is a function of the physical dimensions and hydraulic properties of the aquifer [*Brutsaert and Nieber*, 1977]. Here geometric similarity of a unit-width representative rectangular aquifer (such as

[1]Department of Biological and Ecological Engineering, Oregon State University, Corvallis, Oregon, USA.
[2]Now at National Institute of Water and Atmospheric Research, Christchurch, New Zealand.

0043-1397/06/2006WR005080

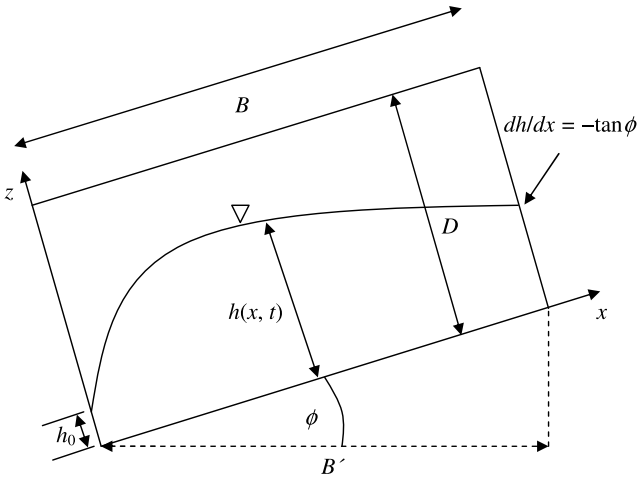

Figure 1. Sketch of a transient water table profile $h(x, t)$ in an inclined aquifer fully incised by a channel at the left-hand side boundary. The water level in the channel is h_0. There is no flux through the right-hand side and bottom boundaries.

that shown in Figure 1) distributed throughout a catchment is assumed, so that the total outflow Q is the integration of all flow q per unit width of aquifer entering a stream network of length L, i.e., $Q = 2qL$ [*Brutsaert and Nieber*, 1977]. The total catchment aquifer area A is equal to $2BL$, where B is the characteristic hillslope length from stream to ridge. Plotted as $\log(-dQ/dt)$ versus $\log(Q)$, equation (2) appears as a straight line with slope b and intercept a. Theoretically, one can fit a line of slope b to recession flow data graphed in this manner and determine aquifer characteristics from the resulting value of a, though care needs to be taken when interpreting plots made from measured data [*Rupp and Selker*, 2006].

[5] In reality, not all recession slope curves will fall along a single curve. This is due in part to concurrent hydrological processes other than groundwater flow, such as overland flow, quick subsurface flow (e.g., macropore flow), decline in channel or reservoir storage, and evapotranspiration [*Brutsaert and Nieber*, 1977]. The combination of these processes will result in a faster rate of decline in discharge for a given discharge than groundwater flow alone. For this reason, it has been suggested that a curve be fit to the lower envelope of the data [*Brutsaert and Nieber*, 1977]. In addition to the above processes, spatial and temporal variability in initial conditions (i.e., initial water table profile) will also result in variability among recession slope curves.

[6] In contrast to the number of studies cited above which compared data to the solutions for the horizontal Boussinesq aquifer, there has been only one attempt to interpret the parameters of recession slope curves based on a solution to the 1-D Boussinesq equation for a sloping rectangular aquifer or hillslope [*Zecharias and Brutsaert*, 1988b], such as that shown in Figure 1. *Zecharias and Brutsaert* [1988b] made the critical assumption that the water table height could be approximated by an effective water table height constant in time and space, thus linearizing the differential equation.

[7] This paper is a partial assessment of the Brutsaert and Nieber method of recession analysis for sloping aquifers. There are two main objectives. The first is to see if recession discharge as predicted by the nonlinear Boussinesq equation for a sloping aquifer is well suited to the Brutsaert and Nieber method and specifically, if the recession curves take the form of (2). Furthermore, as the method relies on analytical solutions, we evaluate existing analytical solutions in their ability to reproduce the solutions to the nonlinear equation when plotted as $\log(-dQ/dt)$ versus $\log(Q)$.

[8] The second objective is to examine how incorporating vertical heterogeneity in saturated hydraulic conductivity k affects the recession discharge from a sloping aquifer. This is of interest because many studies of saturated hydraulic conductivity at the scale of soil samples [e.g., *Harr*, 1977; *Bonell et al.*, 1981; *Beven*, 1982a, 1984] and of lateral saturated conductivity at the hillslope scale [*Brooks et al.*, 2004] have revealed large decreases in k with depth. Specifically, a power law function describing the continuous change in k with height z above bedrock is incorporated into the Boussinesq equation [e.g., *Beven*, 1982b; *Rupp and Selker*, 2005] and solved numerically.

2. Review of Analytical Solutions

[9] For flow in an unconfined aquifer overlaying an impermeable base of slope ϕ, *Boussinesq* [1877] made use of the Dupuit-Forchheimer approximation to derive

$$q = -kh[\cos\phi(\partial h/\partial x) + \sin\phi], \tag{3}$$

where q is the flow rate per unit width of aquifer in the x direction, k is the saturated hydraulic conductivity in the direction parallel to the impermeable layer, and $h = h(x, t)$ is the thickness of the water layer perpendicular to the impermeable layer (see Figure 1). Inserting (3) into the continuity equation yields, in the absence of recharge or evaporation,

$$\varphi\frac{\partial h}{\partial t} = \cos\phi\frac{\partial}{\partial x}\left(kh\frac{\partial h}{\partial x}\right) + \sin\phi\frac{\partial}{\partial x}(kh), \tag{4}$$

where φ is the drainable porosity [see also *Childs*, 1971]. Equation (4) is often expressed for constant k, in which case k is brought outside of the derivative.

[10] Existing analytical solutions to (4) for a horizontal and a sloping aquifer are reviewed below. All the solutions either take the form of (2) exactly, or when b is a function of time, they converge to (2) as t goes to infinity and, in many cases, as t goes to zero. The definitions of the recession parameters a and b in (2) for each solution are listed in Figures 2 and 3. While the following information for a horizontal aquifer is available elsewhere in the published literature, it is useful to have it compiled. More important, to our knowledge this is the first time that most of the analytical solutions for a sloping aquifer have been presented in the form of (2).

2.1. Horizontal Aquifer

[11] For the case of a horizontal aquifer ($\phi = 0$), several analytical solutions to (4) can be presented exactly in the form given by the power law in (2) [*Brutsaert and Nieber*,

Definitions of parameters a and b in $-\frac{dQ}{dt} = aQ^b$ for a horizontal aquifer

Form of Boussinesq Equation†	Time Domain	b	a‡	Parameter Set	Source
Non-linear	Early	3	$\frac{1.133}{k\varphi D^3 L^2}$	(i)	*Polubarinova-Kochina* [1962]
Non-linear	Early	3	$\frac{f_{Lo}}{k\varphi(h_0 - D)^2(h_0 + D)L^2}$	(ii)	*Lockington* [1997]
Non-linear; $k(z) = k_D(z/D)^n$	Early	3	$\frac{f_{R1}}{k_D\varphi D^3 L^2}$	(iii)	*Rupp and Selker* [2005]
Non-linear	Late	3/2	$\frac{4.804k^{1/2}L}{\varphi A^{3/2}}$	(iv)	*Boussinesq* [1904]
Non-linear; $k(z) = k_D(z/D)^n$	Late	$\frac{2n+3}{n+2}$	$\frac{f_{R2}}{\varphi}\left[\frac{k_D L^2}{2^n(n+1)D^n A^{n+3}}\right]^{\frac{1}{n+2}}$	(v)	*Rupp and Selker* [2005]
Linearized	Late	1	$\frac{\pi^2 pkDL^2}{\varphi A^2}$	(vi)	*Boussinesq* [1903]

†Unless specified, k = constant.

‡See Appendix for definitions of f_{Lo}, f_{R1} and f_{R2}

Figure 2. Analytical solutions to various forms of the Boussinesq equation for a horizontal aquifer.

1977]. Beginning with an initially saturated aquifer subjected to instantaneous drawdown, *Polubarinova-Kochina* [1962] derived an exact solution to (4) for a homogeneous and infinitely wide aquifer, which is applicable for early time when the zero-flux boundary at $x = B$ has no effect on the discharge rate. The parameters a and b for this solution, when expressed in the form of (2), are given in Figure 2 (see parameter set i). In this case, the head h_0 at the discharge boundary or channel is assumed to be zero. *Lockington* [1997] arrived at a more general, albeit approximate, early-time solution for any constant value of h_0 between 0 and the initial horizontal water table height D (see set ii in Figure 2). Most recently, *Rupp and Selker* [2005] solved (4) for the early-time domain for an aquifer in which k increases with height z as the following power law (Figure 4):

$$k(z) = k_D(z/D)^n, \tag{5}$$

where k_D is the saturated hydraulic conductivity at height $z = D$, and n is a constant greater than or equal to 0 (see parameter set iii in Figure 2). Note from Figure 2 that the recession slope parameter b equals 3 for each of these three early-time solutions regardless of the head at the aquifer outlet or the vertical distribution of k.

[12] For late times, defined to be when the up-slope zero-flux boundary is influencing the discharge at the drainage boundary, *Boussinesq* [1904] provided an exact solution for a homogeneous aquifer (see parameter set iv in Figure 2). *Rupp and Selker* [2005] later generalized the solution to include the power law k-profile in (5) (see parameter set v in Figure 2). For both solutions, $h_0 = 0$. Note that the recession slope parameter b equals 3/2 for the power $n = 0$ (a homogeneous aquifer) and approaches the value of 2 as n goes to infinity (see Figure 2).

[13] *Parlange et al.* [2001] derived an approximate solution to (4) that unites both the early and late-time solutions for a homogeneous aquifer with $h_0 = 0$.

[14] The early-time ($b = 3$) and late-time ($b = 3/2$) behaviors predicted by the Boussinesq equation for a homogeneous aquifer where $h_0 \approx 0$ have been corroborated by laboratory tank experiments (i.e., Hele Shaw models) [*Ibrahim and Brutsaert*, 1965; *Hammad et al.*, 1966; *Ibrahim and Brutsaert*, 1966; *Mizumura*, 2002, 2005].

[15] An approximate solution given by *Boussinesq* [1903] for the homogeneous aquifer, also limited to late times, can be obtained by linearization of (4) (see parameter set vi in Figure 2). In this case, the variable h outside of the brackets in (3) is set equal to a constant effective water table height pD, where $0 < p \leq 1$. However, the linearization yields a value of 1 for b, which is inconsistent with the laboratory findings cited in the previous paragraph. The linearization is more appropriate when the drop in head at the outflow boundary is much less than the initial saturated thickness of the aquifer, i.e., $D - h_0 \ll D$. This condition has been shown to yield $b = 1$ in late time [e.g., *Szilagyi*, 2004; *van de Giesen et al.*, 2005].

[16] This method of linearization mentioned above is used to arrive at many of the solutions for a sloping aquifer reviewed in the following section. The significance of the linearization parameter p is also discussed in the following section.

2.2. Sloping Aquifer

[17] Numerous transient analytical solutions exist to the Boussinesq equation based on the kinematic wave approximation [*Henderson and Wooding*, 1964; *Beven*, 1981, 1982b] and various approaches to linearization [*Zecharias and Brutsaert*, 1988b; *Sanford et al.*, 1993; *Brutsaert*, 1994; *Steenhuis et al.*, 1999].

[18] The kinematic wave equation arises from assuming that in (3) the hydraulic gradient at any point x is equal to the bed slope, or $dh/dx = 0$, and thus $q = -kh \sin \phi$. This results in the loss of the second-order diffusive term in (4), making it applicable only for steep slopes and/or highly conductive aquifers relative to the recharge rate [*Henderson*

Definitions of parameters a and b in $-\frac{dQ}{dt} = aQ^b$ for a sloping aquifer

Form of Boussinesq Equation[†]	Time Domain	b	a	Parameter Set	Source
Kinematic wave; initially saturated; $k(z) = k_D(z/D)^n$	All	0	0	(vii)	*Beven* [1982b]
Kinematic wave; initially steady-state; $k(z) = k_D(z/D)^n$	All	$\frac{n}{n+1}$	$(n+1)^{n/(n+1)}\frac{N}{\varphi}\left(\frac{2k_D L\sin\phi}{D^n}\right)^{1/(n+1)}$	(viii)	*Beven* [1982b]
Linearized	Late	1	$\frac{8pkDL^2}{\varphi A^2}\left(1+\frac{\eta}{p}\right)$	(ix)	*Zecharias and Brutsaert* [1988b]
Linearized	Late	1	$\frac{8kDL^2}{\varphi A^2}\cos\phi$	(x)	*Sanford et al.* [1993]
Linearized	Late	3/2	$\frac{6.928k^{1/2}L}{\varphi A^{3/2}}\left(1+\frac{3}{4}\eta\right)^{-1/2}$	(xi)	*Sanford et al.* [1993]
Linearized	Early	3/2	$\frac{6.928\,k^{1/2}L}{\varphi A^{3/2}}\cos^{1/2}\phi\left\{\frac{1+\eta/4}{[1+(\eta/2)]^{-1/2}}\right\}$	(xii)	*Sanford et al.* [1993]
Linearized	Late	1	$\frac{6kDL^2}{\varphi A^2}\eta\cos\phi$	(xiii)	*Sanford et al.* [1993]
Linearized	Late	1	$\frac{8kDL^2}{\varphi A^2}\eta^2\cos\phi$	(xiv)	*Steenhuis et al.* [1999]
Linearized	Early	3	$\frac{1.133}{k\varphi D^3L^2\cos\phi}$	(xv)	*Brutsaert* [1994]
Linearized	Late	1	$\frac{\pi^2 pkDL^2}{\varphi A^2}\cos\phi\left[1+\left(\frac{\eta}{\pi p}\right)^2\right]$	(xvi)	*Brutsaert* [1994]
Non-linear	Late	1	$\frac{200kL}{\varphi A}\sin\phi$	(xvii)	[‡]
Non-linear; $B\tan\phi < h_0$	Late	1	$\frac{\pi^2 kh_0L^2}{\varphi A^2}\cos\phi\left(1-\frac{B\tan\phi}{2h_0}\right)$	(xviii)	[‡]
Non-linear; $k(z) = k_D(z/D)^n$	Late	$\frac{2n+1}{n+1}$	$\frac{(n+1)^2}{(n+.01)\varphi A}\left[\frac{2k_D L\sin\phi}{(n+1)D^n}\right]^{\frac{1}{n+1}}$	(xix)	[‡]

[†]Unless specified, $k(z)$ = constant and $h_0 = 0$
[‡]This article.

Figure 3. Analytical solutions to various forms of the Boussinesq equation for a sloping aquifer.

and Wooding, 1964]. As there is no diffusion, the entire recession slope curve is defined by the initial shape of the water table. For an initially saturated aquifer with the power law k profile in (5), it can be shown that the kinematic wave equation predicts a recession discharge that is constant in time [*Beven*, 1982b]:

$$Q = 2k_D DL\sin\phi/(n+1). \tag{6}$$

Thus $dQ/dt = 0$ for all Q and the recession constants a and b both effectively equal 0 (see set vii in Figure 3). On the other hand, beginning with a steady state water table profile following a period of constant and spatially uniform recharge N, the recession constant b equals 0 for a homogeneous aquifer and approaches 1 as n approaches infinity (see set viii in Figure 3).

[19] Another approach to making (4) more tractable is to use the quasi steady state assumption that the shape of the moving water table is the same as that calculated for steady flow. *Zecharias and Brutsaert* [1988b] made this assumption along with the linearization discussed above to obtain a solution for a sloping homogeneous aquifer (see set ix in Figure 3). Note the resemblance of the recession parameter a given in Figure 3 to the definition of a for a linearized horizontal aquifer (see set vi in Figure 2). The two are nearly equivalent but for a "slope factor" which contains the dimensionless term η:

$$\eta = \frac{B}{D}\tan\phi. \tag{7}$$

This way of expressing a as the horizontal parameterization multiplied by a slope factor is also done, when appropriate, for several other solutions reviewed below. Though it does not generally result in the simplest form for a, it facilities the comparison of the various solutions. The parameter η is identical to the "groundwater hillslope flow number" defined by *Brutsaert* [2005] for $p = 1$. This number

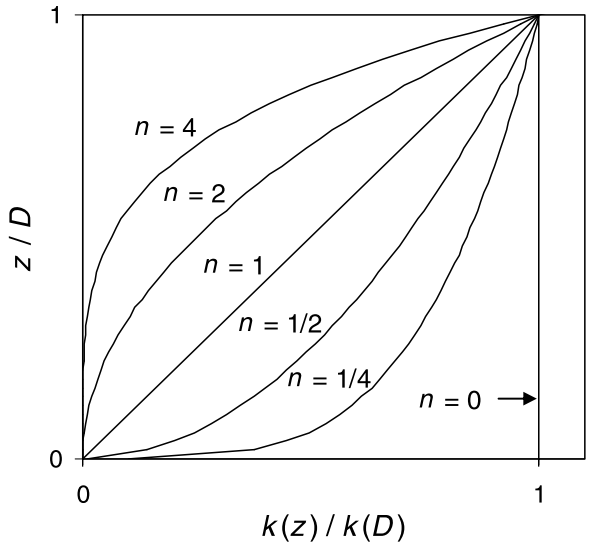

Figure 4. Examples of saturated hydraulic conductivity (k) profiles in an aquifer of thickness D where k is proportional to the height z to a power n.

"represents the relative magnitude of the slope term, i.e., gravity, versus the diffusion term" [*Brutsaert*, 1994].

[20] Using a similar quasi steady state approach, *Sanford et al.* [1993] presented three solutions for cumulative discharge, each based on a different method for approximating the effective water table height. We refer the reader to *Sanford et al.* [1993] for a description of the three approximations used. The three solutions are presented in the form of (2) for the case where $h_0 = 0$ for comparison with the other solutions presented herein. The first two solutions yield a constant value of the recession constant b (1 and 1.5, respectively) (see sets x and xi in Figure 3). The third solution differs in that the value of b transitions in time from 1.5 to 1 (see sets xii and xiii in Figure 3).

[21] *Steenhuis et al.* [1999] addressed the conditions of the steep hillslope experiments at the Coweeta Hydrological Laboratory. For their solution, $h_0 = D$ and the initial water table is a straight line with boundaries $h(0, 0) = D$ and $h(B, 0) = 0$. The solution can be expressed as

$$\frac{dQ}{dt} = -\frac{2Q(Q - kDL\sin\phi)^2}{\varphi k D^3 L^2 \cos\phi}. \tag{8}$$

It can be shown that as t goes to infinity, (8) converges to the form of (2) with the recession parameter b equal to 1 (see set xiv in Figure 3).

[22] *Brutsaert* [1994] used a linearization in h to arrive at an infinite series summation solution for an instantaneous drawdown to $h(0, t) = 0$ in an initially saturated homogeneous aquifer. It can be shown [*Brutsaert and Lopez*, 1998] that as t goes to zero the early-time value of b goes to 3 (see set xv in Figure 3). For late time, the solution can also be expressed as (2) by neglecting all but the first term in the summation in equation (17) of *Brutsaert* [1994] (see set xvi in Figure 3).

[23] Others have used the same linearization approach as *Brutsaert* [1994], but have included variable recharge rates, nonzero stream water levels, and constant head at the upslope boundary [*Verhoest and Troch*, 2000; *Pauwels et al.*, 2002; *Verhoest et al.*, 2002; *Pauwels et al.*, 2003]. *Chapman* [1995] also addressed a pulse of recharge but rewrote (4) for h^2 and used a linearization in h^2 to arrive at a solution. Though these solutions differ from *Brutsaert* [1994] in early time due to different initial conditions, it can be shown that they are essentially equal in the late time domain (b and a are given by set xvi in Figure 3) for the zero-flux upslope boundary condition.

[24] One can see from Figure 3 that $b = 1$ for all but one of the linearized late-time solutions for a homogeneous aquifer. In experiments using an inclined Hele Shaw model, *Mizumura* [2005] observed that at late time the discharge declined exponentially with time, which is equivalent to $b = 1$.

[25] It is worth briefly discussing the parameter p that arises from the linearization method employed by *Brutsaert* [1994] and others [*Zecharias and Brutsaert*, 1988b; *Chapman*, 1995; *Verhoest and Troch*, 2000; *Pauwels et al.*, 2002]. The assumption of the linearization is that changes in the water table height are small such that a constant "effective" water table of height equal to pD can be assumed. Though this method has yielded analytical solutions to the Boussinesq equation, it leads to one more parameter for which to solve. It has been suggested that p be treated as a calibration parameter [*Brutsaert*, 1994], but this not desirable if the goal is to identify the value of other unknowns, such as k and φ.

[26] For an initially saturated aquifer, *Brutsaert* [1994] points out that previous analytical solutions for a horizontal aquifer suggest a relatively narrow range of values for p between 1/3 and 1/2. However, an initially saturated unconfined aquifer will not often occur in natural conditions [*van de Giesen et al.*, 2005], so the determination of p is not straightforward. Where the aquifer is sloping, *Koussis* [1992] proposed the following implicit equation for pD for the special case of a steady state water table profile due to a constant recharge rate N and a channel head $h_0 = 0$:

$$\frac{B\tan\phi}{2pD} = \frac{k\sin^2\phi}{N} + \frac{pD}{B\tan\phi} - \left(\frac{pD}{B\tan\phi} + 1\right)\exp\left(-\frac{B\tan\phi}{pD}\right). \tag{9}$$

Table 1. Parameter Values Used in Numerical Simulations

Parameter	Value	
	Homogeneous Aquifer ($n = 0$)	Heterogeneous Aquifer ($n > 0$)
k_D [m d^{-1}]	1, 10, 50	10, 100
φ	0.01, 0.1	0.1, 0.2
$\tan\phi$	0.00125–1.281	0.003, 0.03, 0.3
B [m]	9–147	50, 200
D [m]	1, 2	0.25, 1
n	0	0.0625–64
$k_D \sin\phi/((n+1)\varphi B)$ [d^{-1}]	0.006–7.9	0.0012–2.9
$\eta = B\tan\phi/D$	0.0625–64	0.15–60
h_0/D	0, 0.5, 1	0
N/k[a]	0.002	...
Total runs	55	20

[a]Only for steady state initial condition.

Though (9) is slightly cumbersome, explicit approximations can be derived that are applicable for given ranges of η [*Koussis*, 1992].

3. Methods

3.1. Numerical Solution of the Boussinesq Equation

[27] The subsurface flow in a sloping aquifer with a power law k profile can be expressed as

$$q = -\frac{k_D D}{n+1}(h/D)^{n+1}[\cos\phi(\partial h/\partial x) + \sin\phi]. \tag{10}$$

Note that k has been replaced by $k(h)$ in (3) where

$$k(h) = \frac{k_D}{(n+1)}(h/D)^n. \tag{11}$$

The corresponding transient water table height is

$$\frac{\partial h}{\partial t} = \frac{k_D}{\varphi(n+1)D^n}\left[\cos\phi\frac{\partial}{\partial x}\left(h^{n+1}\frac{\partial h}{\partial x}\right) + \sin\phi\frac{\partial}{\partial x}\left(h^{n+1}\right)\right] + \frac{N}{\varphi} \tag{12}$$

for a recharge rate N. Equation (12) was solved numerically using a fourth-order Runge-Kutta finite difference method. A zero-flux condition was maintained on the upslope boundary.

[28] A total of 75 model runs have been reported. For 55 of the runs, the aquifer was homogeneous ($n = 0$). Of these, 45 simulated the drainage of an aquifer initially saturated to a uniform height D, and the remaining 10 simulated drainage following steady state recharge conditions. For the steady state cases, an initial steady state water table profile was generated by applying a constant and spatially uniform recharge rate N to an initially dry aquifer until the discharge rate q reached 99.99% of the recharge rate NB. Also, 35 of the 55 runs were subjected to complete drawdown at the channel ($h_0 = 0$), while for 20 runs h_0 was set at $0.5D$ or D. The model parameters k_D, φ, $\tan\phi$, B, and D were varied as indicated in Table 1.

[29] Twenty model runs corresponded with a heterogeneous aquifer, with the power n ranging from 0.0625 to 64 (see, e.g., Figure 4). Only the initially saturated case for $h_0 = 0$ was simulated. The values of remaining model parameters are given in Table 1.

3.2. Dimensional Analysis

[30] In order to generalize the results of the model runs, transient discharge was expressed without dimension where an appropriate manner of scaling both time and discharge were known. Below is presented the manner in which transient discharge was scaled for the case where $h_0 = 0$. As the authors could not find a meaningful way to scale time and discharge for $h_0 > 0$, transient discharge was left unscaled for this boundary condition.

3.2.1. Initially Saturated Aquifer

[31] When aquifer discharge is diffusion-controlled, such as at early time or for small η, dimensionless time t^*_d and dimensionless discharge Q^*_d are given as

$$t^*_d = \frac{\mathrm{B}^2_{R2}k_D D\cos\phi}{2(n+3)\varphi B^2}t \tag{13}$$

$$Q^*_d = \frac{(n+1)(n+3)B}{2\mathrm{B}_{R2}k_D D^2 L\cos\phi}Q, \tag{14}$$

where the subscript d denotes diffusion dominance. Equations (13) and (14) are based on the analytical solution of (12) given an initially saturated horizontal aquifer [*Rupp and Selker*, 2005] with an additional typically minor aquifer slope adjustment of $\cos\phi$ [see *Brutsaert*, 2005, pp. 409–411]. Integrating (13) by (14) yields the dimensionless time rate of change in discharge

$$\frac{dQ^*_d}{dt^*_d} = \frac{(n+1)(n+3)^2\varphi B^3}{\mathrm{B}^3_{R2}k^2_D D^3 L\cos^2\phi}\frac{dQ}{dt}. \tag{15}$$

[32] When aquifer discharge is gravity-controlled (late time or large η), dimensionless time and discharge arise from consideration of the celerity of the kinematic wave [e.g., *Brutsaert*, 2005, equation (10.151)] adjusted for the vertical k profile, and a characteristic length B, such that dimensionless time is

$$t^*_g = \frac{k_D\sin\phi}{(n+1)\varphi B}t \tag{16}$$

and dimensionless discharge is

$$Q^*_g = \frac{n+1}{2k_D DL\sin\phi}Q, \tag{17}$$

where the subscript g denotes gravity dominance. The corresponding dimensionless time rate of change in discharge is

$$\frac{dQ^*_g}{dt^*_g} = \frac{(n+1)^2\varphi B}{2k^2_D DL\sin^2\phi}\frac{dQ}{dt}. \tag{18}$$

[33] We arrive at a dimensionless time for when both diffusion and gravity are important by combining (13) and (16) as

$$t^* = \frac{k_D}{\varphi B}\left(\frac{\mathrm{B}^2_{R2}D\cos\phi}{2(n+3)B} + \frac{\sin\phi}{n+1}\right)t. \tag{19}$$

Dimensionless discharge is similarly formed from (14) and (17) as

$$Q^* = \frac{1}{2k_D DL}\left[\frac{\mathrm{B}_{R2}D\cos\phi}{(n+1)(n+3)B} + \frac{\sin\phi}{n+1}\right]^{-1}Q, \tag{20}$$

and the dimensionless time rate of change in discharge is

$$\frac{dQ^*}{dt^*} = \frac{\varphi B}{2k^2_D DL}\left(\frac{\mathrm{B}_{R2}D\cos\phi}{(n+1)(n+3)B} + \frac{\sin\phi}{n+1}\right)^{-1} \cdot\left(\frac{\mathrm{B}^2_{R2}D\cos\phi}{2(n+3)B} + \frac{\sin\phi}{n+1}\right)^{-1}\frac{dQ}{dt}. \tag{21}$$

3.2.2. Initially Steady State; $n = 0$

[34] For initially steady state conditions, we did not have a solution to the nonlinear Boussinesq equation to provide

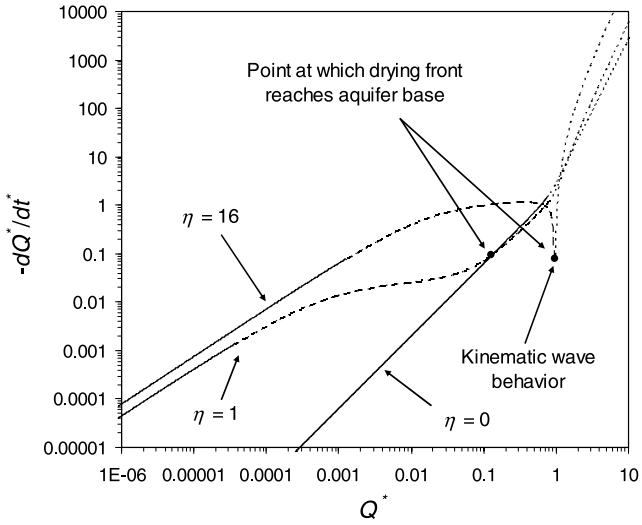

Figure 5. Numerically generated recession slope curves predicted by the nonlinear Boussinesq equation for an initially saturated homogeneous aquifer subjected to full and instantaneous drawdown at the downhill boundary. The dotted, dashed, and solid sections of each curve correspond to the early, intermediate, and late-time domains, respectively, described in the text. Also indicated is the point on each curve where the drying front first reaches the aquifer base at the uphill aquifer boundary. The three curves are for aquifers with gradients of 0, 2, and 32%.

an obvious manner for arriving at a dimensionless time for conditions of diffusion dominance as in (13). We replaced the initial saturated thickness D in (13) with the maximum height $h_{\max}$ of the steady state water table in a horizontal aquifer. For $h_0 = 0$ and $n = 0$, $h_{\max} = B\sqrt{N/k}$ [e.g., *Rupp and Selker*, 2005]. Dispensing furthermore with the term $B_{R2}^2/[2(n + 3)]$ leads to

$$t_d^* = \frac{k\cos\phi}{\varphi B}\left(\frac{N}{k}\right)^{1/2} t. \tag{22}$$

Dimensionless discharge is discharge divided by the uniform recharge rate:

$$Q_d^* = \frac{1}{2NBL}Q. \tag{23}$$

For gravity-controlled conditions, dimensionless time t^*_g is given by (16) with $n = 0$, while dimensionless discharge Q^*_g is again equal to (23). When both diffusion and gravity are factors, dimensionless time and discharge are

$$t^* = \frac{k}{\varphi B}\left(\cos\phi\sqrt{\frac{N}{k}} + \sin\phi\right)t \tag{24}$$

$$Q^* = \frac{1}{2NBL}Q, \tag{25}$$

respectively, and the dimensionless time rate of change in discharge is

$$\frac{dQ^*}{dt^*} = \frac{\varphi}{2kNL}\left(\cos\phi\sqrt{\frac{N}{k}} + \sin\phi\right)^{-1}\frac{dQ}{dt}. \tag{26}$$

4. Results and Discussion

4.1. Comparison of Numerical and Analytical Solutions for Homogeneous Aquifer

4.1.1. Discharge Boundary Head (h_0) = 0

[35] First we review the case of a horizontal aquifer. The solution for discharge from an initially level water table subjected to an instantaneous drop in head to 0 at the outflow boundary can be separated into two very distinct temporal domains separated by a sharp transition when plotted as $\log(-dQ/dt)$ versus $\log(Q)$ [e.g., *Parlange et al.*, 2001] (see also Figure 5 for $\eta = 0$). The recession slope curve in each of these domains follows its well-known behavior: as a straight line with slope $b = 3$ and 3/2 for the early and late time, respectively. The early-time domain corresponds to the period during which the water table height h at the no-flux boundary at $x = B$ remains fixed at its initial height, i.e., $h(B, t) = D$. During the late-time domain, the water table is moving downward at the no-flux boundary. For other initial conditions this distinct early-time pattern for which $b = 3$ may be absent (see, e.g., Figure 6 for $\eta = 0$) and the transition to the late time domain may look different [*van de Giesen et al.*, 2005].

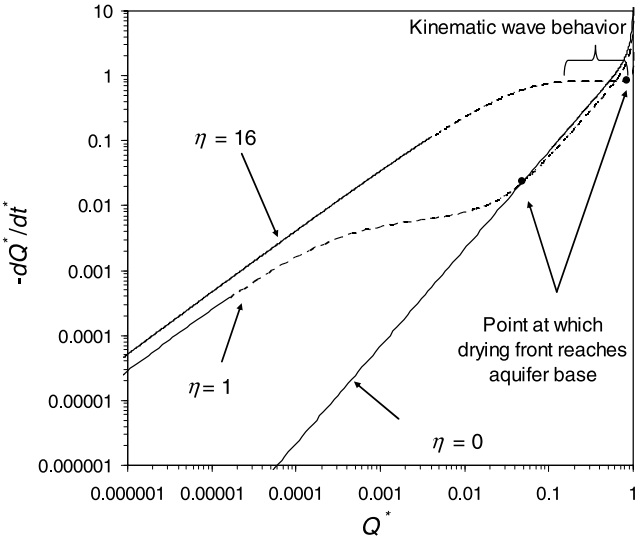

Figure 6. Numerically generated recession slope curves predicted by the nonlinear Boussinesq equation for a homogeneous initially steady state aquifer with water height = 0 at the downhill boundary. The dashed and solid sections of each curve correspond to the intermediate and late-time domains, respectively, described in the text. Also indicated is the point on each curve where the drying front first reaches the aquifer base at the uphill aquifer boundary. The three curves are for aquifers with gradients of 0, 2, and 32%.

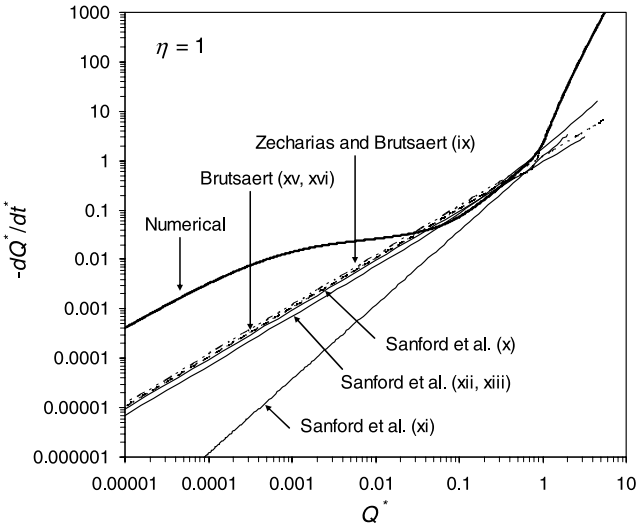

Figure 7. Recession slope curves predicted by several analytical solutions to the Boussinesq equation for a mildly sloping homogeneous aquifer. Also shown is the numerical solution of an initially saturated aquifer subjected to an instantaneous drop to 0 in channel head h_0. For all solutions, $\tan\phi = 0.02$, $D = 1$ m, $B = 50$ m, $L = 1$ m, $k = 50$ m d^{-1}, and $\varphi = 0.1$. The roman numerals correspond to the recession parameters for each curve given in Figure 3.

[36] In the case of the sloping aquifer the water table at both the channel ($x = 0$) and the ridge line ($x = B$) begins to drop immediately, forming a "mound" (see Figure 1) which progresses downslope. Additionally, the water table eventually reaches the aquifer base at $x = B$ and the point x at which $h = 0$ recedes downslope [*Stagnitti et al.*, 2004]. The result is a more complex discharge pattern than seen for the horizontal aquifer. Still visible is an early-time domain in which the recession slope curve has a nonconstant slope b greater than 3 which approaches infinity for steep slopes (see Figure 5). Also for steep slopes (e.g., $\eta > 16$), the period when b reaches a maximum is when the body of water is behaving as a kinematic wave. Though there may be considerable drainage during this period, the discharge rate changes little, and thus it appears hardly as more than a point in a plot of $\log(-dQ/dt)$ versus $\log(Q)$. In contrast, for mildly sloping aquifers the transition out of the early-time domain is similar to the transition from early to late time in a horizontal aquifer.

[37] Following the early-time domain, there is an intermediate domain which bridges the early- and late-time domains. The particular shape of the intermediate domain depends greatly on the aquifer slope (see Figure 5). From the intermediate time there follows a transition to the late time in which the curves converge to the form of (2) with $b = 1$. However, this transition occurs after much of the aquifer has already drained and long after the water table has begun to recede downslope along the aquifer base.

[38] When the water table is initially at steady state due to a constant recharge rate, the early-time domain all but disappears (Figure 6) and there is a quick transition to the intermediate domain. For steep aquifers, the intermediate domain is characterized by a "plateau" where the time rate of change in discharge is constant and then gradually transitions to the late time where (2) holds (Figure 6). This plateau corresponds to the kinematic wave behavior. For mildly sloping aquifers, the intermediate time is at first much like the late time of the horizontal aquifer. Eventually, all the curves transition to the late-time domain, similar to the initially saturated case.

[39] Despite the complex shapes of the recession curves shown Figures 5 and 6, a Brutsaert and Nieber–type analysis may still be applicable, particularly when quality low-flow data are available, so long as appropriate analytical solutions are available.

[40] However, the analytical solutions reviewed in section 2.2 are not consistent with the numerical solutions to the nonlinear equation, nor are they consistent among themselves, particularly as the slope ϕ (or η) increases. Figures 7 and 8 show the recession slope curves for several solutions given equivalent values for the parameters B, D, L, k, φ, and, where present, p. For mild slopes ($\eta < 1$), many of the solutions are similar, and differences can largely be accounted for by the constant in the recession parameter a: For example, the value of 8 in set ix versus the value of π^2 in set xvi in Figure 3. An exception is the second equation of *Sanford et al.* [1993] (see parameter set xi), for which b has the value of 3/2. As the slope ϕ or η increases, the analytical solutions diverge greatly (see Figure 8).

[41] Because the linearized solution of *Brutsaert* [1994] encompasses the early- through late-time behavior of the numerical solution, it was examined most closely. The similarly derived analytical solution of *Verhoest and Troch* [2000] given a water table initially at steady state was also assessed. For the remainder of this section, references to the "linearized solution" refer only to those solutions following Brutsaert's solution [*Brutsaert*, 1994; *Verhoest and Troch*, 2000; *Pauwels et al.*, 2002].

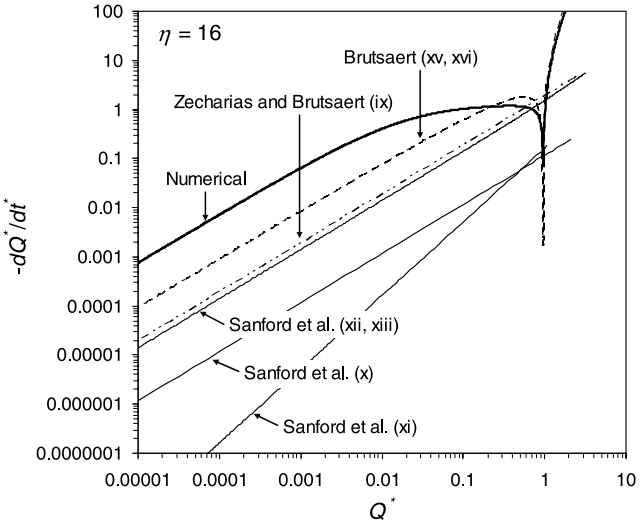

Figure 8. Recession slope curves predicted by several analytical solutions to the Boussinesq equation for a moderately sloping homogeneous aquifer. Also shown is the numerical solution of an initially saturated aquifer subjected to an instantaneous drop to 0 in channel head h_0. For all solutions, $\tan\phi = 0.32$, $D = 1$ m, $B = 50$ m, $L = 1$ m, $k = 50$ m d^{-1}, and $\varphi = 0.1$. The roman numerals correspond to the recession parameters for each curve given in Figure 3.

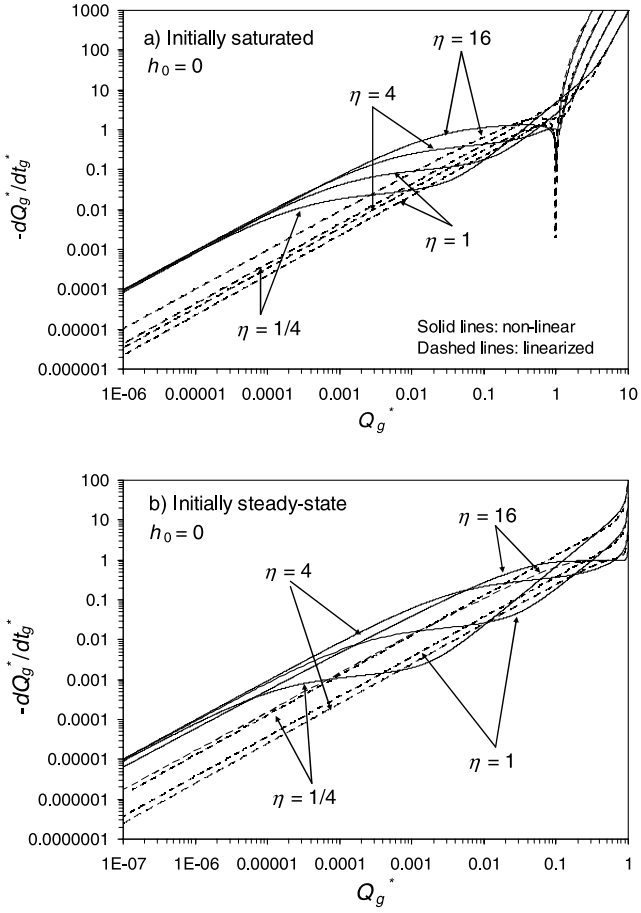

Figure 9. Comparison of numerical solutions (solid lines) of the nonlinear Boussinesq equation with analytical solutions (dashed lines) of the linearized Boussinesq equation following (a) *Brutsaert* [1994] and (b) *Verhoest and Troch* [2000]. The solutions are for a homogeneous aquifer with discharge boundary condition $h_0 = 0$ and the following initial conditions: saturation to a height $D = 1$ m (Figure 9a) and steady state discharge due to uniform recharge $N = 0.1$ m d^{-1} (Figure 9b). Recession curves were generated for tan $\phi = 0.005$, 0.02, 0.08, and 0.32. For all solutions, $B = 50$ m, $L = 1$ m, and $k = 50$ m d^{-1}, and $\varphi = 0.1$.

[42] For comparison with the numerical solutions, the linearized solution was given nearly identical parameterization. Because there is not yet a theory for determining p a priori, we let $p = 0.3465$ [*Brutsaert and Nieber*, 1977] for all solutions for an initially saturated aquifer, even though it would seem more appropriate for p to be a function of ϕ. For the initially steady state cases, pD was calculated by (9).

[43] The early time domain in the initially saturated case is well reproduced by the linearized solution (Figure 9). However, the intermediate-time domain of the linearized solution extends over a much narrower range of discharges and the convergence toward a value of $b = 1$ is more rapid than in the numerical result. The significance for aquifer characterization is that the corresponding value of the late-time parameter a in (2) is not the same for the solutions to the nonlinear and linearized equation; in some cases, the value of a differs by an order of magnitude. For mildly sloping aquifers, the linearized solution clearly does not match the numerical solution at intermediate and late times (Figure 9).

[44] Because the analytical solutions to the linearized Boussinesq equation do not match the numerical solutions to the nonlinear equation outside of the early time, we attempted to empirically derive an analytical solution to the nonlinear equation for late time by noting that individual recession slope curves generated with unique parameter values appear to converge upon a single curve when time and discharge are given by the "gravity-controlled" dimensionless quantities given by (16) and (17), respectively (Figure 9). This is true for both the initially saturated aquifer and the initially steady state aquifer, but the convergence appears weaker for the latter case.

[45] The dimensionless late-time recession curve is estimated by

$$dQ_g^*/dt_g^* = a^* Q_g^*, \tag{27}$$

where $a^* \approx 100$. Substituting (17) and (18) into (27) yields

$$dQ/dt = 100\frac{k_D \sin\phi}{\varphi B} Q. \tag{28}$$

Equation (28) is also given in Figure 3 (see parameter set xvii), but with the substitution $B = A/(2L)$ to permit easier comparison with the other solutions in the table. There is a good 1:1 match between a from (28) and the numerically derived values of a (Figure 10). For all but one value, the error is within ±15%; for the other value, which corresponds to the initially steady state case for tan $\phi = 0.32$, the error is −33%.

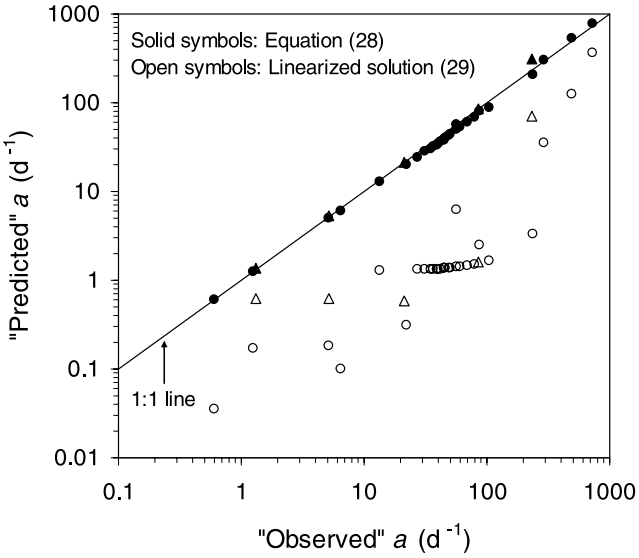

Figure 10. Late-time recession parameter a predicted from equations (28) and (29) plotted against the observed a determined from numerically derived recession slope curves for the case where the head at the discharge boundary (h_0) = 0. The circles correspond to an aquifer initially saturated to a height D, and the triangles correspond to the initially steady state water table due to a uniform recharge rate N. Each numerical simulation had unique set of values of ϕ, φ, k, D, and B.

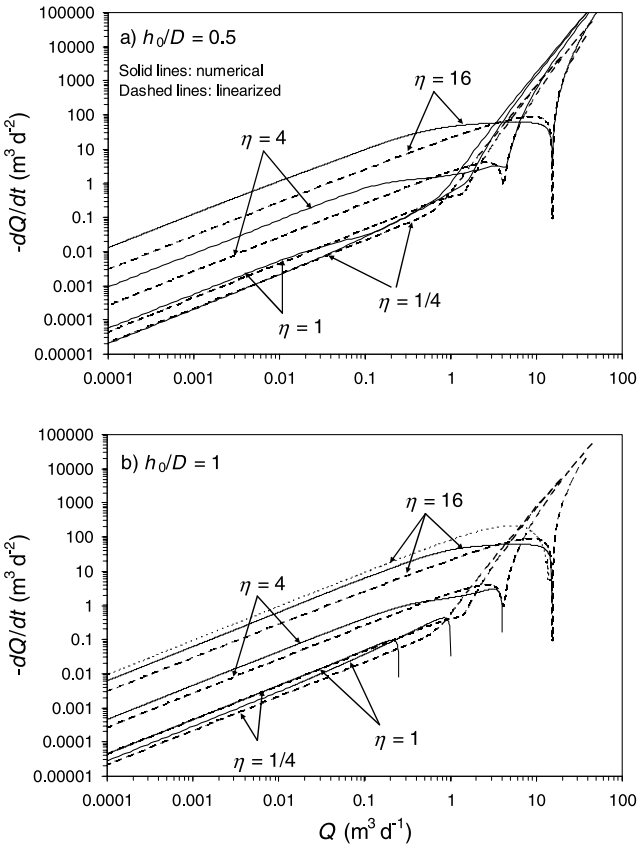

Figure 11. Comparison of numerical solutions (solid lines) of the nonlinear Boussinesq equation with analytical solutions (dashed lines) of the linearized Boussinesq equation following *Brutsaert* [1994]. The solutions are for a homogeneous aquifer with discharge boundary condition $h_0/D = 0.5$ and 1 and initial saturation to a height $D = 1$ m. Recession curves were generated for tan ϕ = 0.005, 0.02, 0.08, and 0.32. For all solutions, $B = 50$ m, $L = 1$ m, and $k = 50$ m d^{-1}, and $\varphi = 0.1$. The solution of *Steenhuis et al.* [1999] is also shown for the steep slope case where $h_0 = D$ (dotted line).

[46] It is worth noting that D, the depth of the aquifer, is absent from (28). This is a useful result with regards to hydraulic parameter estimation as it eliminates the problem of uncertainty in knowing D in the field. It is also interesting that B appears in (28) even though by this time the upslope end of the water table is traveling down the aquifer base. This implies that although the water body is no longer in contact with the boundary at $x = B$, it retains the memory of its presence for an indefinite period.

[47] Obviously the most striking difference between (28) and any of the linearized solutions given in Figure 3 is the curiously large constant of "100." We can offer no explanation for how this value arises, but its significance with respect to aquifer parameter estimation is certainly great. The other key difference is that a in (28) varies with aquifer slope in a manner unlike all but one of the linearized solutions in Figure 3. The exception is the third late-time solution of *Sanford et al.* [1993] (see parameter set xiii), which is identical to (28) but for the constant of 100 after making the substitution $\eta = B\tan\phi/D$.

4.1.2. Discharge Boundary Head (h_0) > 0

[48] We examined the effect of a nonzero h_0 as one would expect the linearized solution to perform better for h_0/D near 1. It should be noted that the linearized solutions do not permit the water table to move down the aquifer base after reaching a height of 0 at $x = B$, so how this affects the late time recession curve is certainly of interest [*Stagnitti et al.*, 2004]. Furthermore, the linearized solutions for discharge do not explicitly account for the head at the channel h_0. Interestingly, though h_0 is a parameter in the linearized equation for the transient water table height in the work by *Pauwels et al.* [2002], it is absent from the equation for discharge. One is left then to account for a nonzero value of h_0 through the parameter p. Because there is not yet a theory for determining p a priori, we let $p = 0.3465$ [*Brutsaert and Nieber*, 1977] for all solutions for an initially saturated aquifer, even though it would seem more appropriate for p to be a function of at least h_0 and ϕ. For the initially steady state cases, pD was calculated by (9).

[49] In the early-time domain, the linearized solution appears to do less well for $h_0/D = 0.5$ than for $h_0/D = 0$ at reproducing the nonlinear solution, particularly for mildly sloping aquifers (compare Figures 9a and 11a). Curiously, the linearized solution retains the early-time domain even when $h_0/D = 1$, in contrast with the numerical solution (Figure 11b).

[50] At late time the linearized solutions move closer to the numerical solutions as h_0/D approaches 1 (Figure 11). Again, this is not surprising because the linearization is more suited to conditions where $D - h_0 \ll D$. A more appropriate choice of p for $h_0 > 0$ should bring the solutions even closer together.

[51] Though not shown, the general relationship of a to the aquifer parameters given in (28) does not persist for values of $h_0/D = 0.5$ or 1. As an aid to understanding why this is not so, we plotted a against $B\tan\phi/h_0$. It is clear from Figure 12 that a transition between regimes occurs at $B\tan\phi/h_0 = 1$. When $h_0 > B\tan\phi$, the water table at the upslope boundary never reaches the aquifer base. It is useful to know what the linearized solution of *Brutsaert* [1994] would predict in this regime. Rewriting the definition of a from *Brutsaert* [1994] given in Figure 3 (parameter set xvi) in terms of B gives

$$a = \frac{\pi^2 pkD}{4\varphi B^2}\cos\phi\left[1 + \left(\frac{\eta}{\pi p}\right)^2\right]. \qquad (29)$$

When $h_0 > B\tan\phi$, the term in brackets in (29) is approximately 1 for most realistic conditions and (29) simplifies to the linearized solution for a horizontal aquifer [*Boussinesq*, 1903] with a relatively insensitive slope factor of cos ϕ. What remains uncertain is the value of the effective water table height pD at late time. If we assume that the effective water table height pD is the average height of the water table following an infinitely long time, i.e., when the water table is flat, (29) can be estimated by

$$a \approx \frac{\pi^2 k}{4\varphi B^2}\cos\phi\left(h_0 - \frac{B\tan\phi}{2}\right) \qquad \frac{B\tan\phi}{h_0} \le 1. \qquad (30)$$

Equation (30) is also given in Figure 3 but written in terms of η and A for consistency (see parameter set xviii).

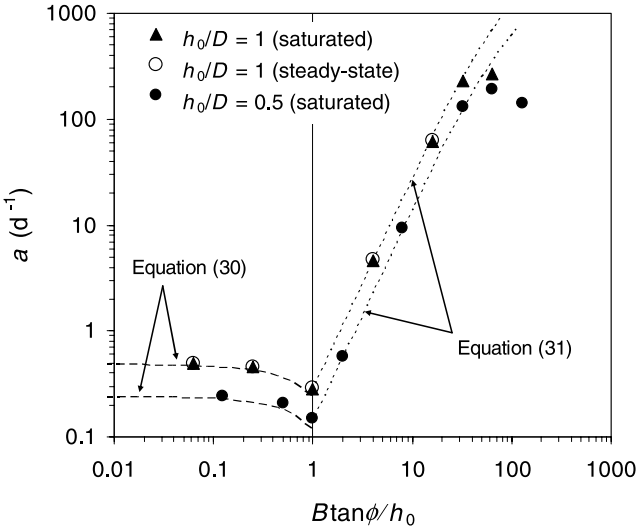

Figure 12. Late-time recession parameter a determined from numerically derived recession slope curves plotted against $B\tan\phi/h_0$, for the case where the water level in the channel h_0 is not zero. Each point corresponds to a drainage simulation of a homogeneous aquifer initially saturated to a depth D with h_0/D = 0.5 or 1, and $\tan\phi$ varying from 0.00125 to 1.28. For each simulation, D = 1 m, B = 50 m, L = 1 m, k = 50 m d^{-1}, and φ = 0.1. Also shown are equations (17) and (18) for h_0 = 1 (dotted) and h_0 = 0.5 (dashed). In (18), the parameter p was set to 0.09 for h_0 = 1 and to 0.18 for h_0 = 0.5.

Though not exact, (30) captures the general behavior seen in Figure 12 remarkably well.

[52] In the other regime where $h_0 < B\tan\phi$, which is most likely to occur when $(\eta/(\pi p))^2 \gg 1$, equation (29) may be simplified to

$$a = \frac{k}{4\varphi pD}\cos\phi\tan^2\phi \qquad 1 < \frac{B\tan\phi}{h_0} < 32. \tag{31}$$

It is evident from Figure 12 that the term $\cos\phi\tan^2\phi$ captures well the dependence of a on aquifer slope, at least for $B\tan\phi/h_0 < 32$. There is insufficient information at this point however, to suggest a function for the effective water table pD. The two curves for (31) shown in Figure 12 were fit visually through the points using pD = 0.09 for $h_0 = D$ and pD = 0.18 for $h_0 = 0.5D$. It appears thus that $1/(pD)$ may be approximated by a linear function of h_0, though at this time we offer no further explanation.

[53] The above analysis reveals that the linearized solutions of *Brutsaert* [1994] and *Verhoest and Troch* [2000] perform poorly outside of the early-time domain for h_0 = 0. This point should be stressed, as it is often this boundary condition that has been used in the literature when assessing the performance of linearized solutions to the Boussinesq equation. On the other hand, the linearized solutions are capturing much of the behavior of the nonlinear Boussinesq equation when h_0/D is at least as great as 0.5. What remains unknown is how to define the parameter p when $h_0 < B\tan\phi$. This corresponds to the condition where the upslope end of water table is moving down the aquifer base, a feature of the nonlinear equation which the linearized solutions do not reproduce.

4.2. Effect of the Power Law Conductivity Profile

[54] The value of the power n determines the shape of the recession slope curve in the intermediate and late times (see Figure 13). As n increases, the intermediate time domain occupies a progressively smaller range of discharges. At late time the dimensionless curves converge to

$$dQ_g^*/dt_g^* = a^*\left(Q_g^*\right)^b, \tag{32}$$

where

$$b = (2n+1)/(n+1) \tag{33}$$

and t^*_g and Q^*_g are calculated by (16) and (17), respectively. In contrast, at early time the curves retain their general shape for a given aquifer slope irrespective of the value of n. This similarity in early time is consistent with the analytical solution for a horizontal aquifer [*Rupp and Selker*, 2005]. It is worth noting that because k decreases to zero at the aquifer base, the possible condition for the homogeneous aquifer in which the water table drops to the aquifer base at the point $x = B$ and then travels downslope does not arise.

[55] A value of a^* was calculated for each value of n by fitting (32) to the numerically generated late time recession curves. Figure 14 shows the numerically derived a^* plotted

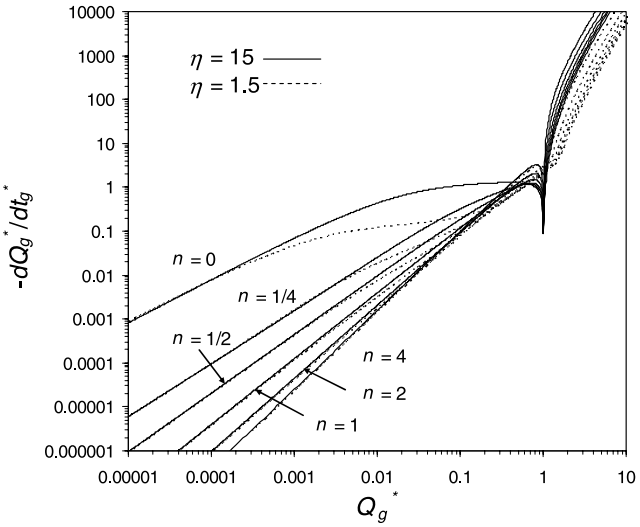

Figure 13. Numerically generated recession slope curves for a mildly ($\tan\phi$ = 0.03, η = 1.5) and moderately ($\tan\phi$ = 0.3, η = 15) sloping aquifer where the saturated hydraulic conductivity profile is a power function of the height above the impermeable base. Shown are curves for various values of the power n. The curves are for an initially saturated aquifer subjected to an instantaneous drop to 0 in channel head h_0. For all curves, D = 1 m, B = 50 m, L = 1 m, k_D = 10 m d^{-1}, and φ = 0.1.

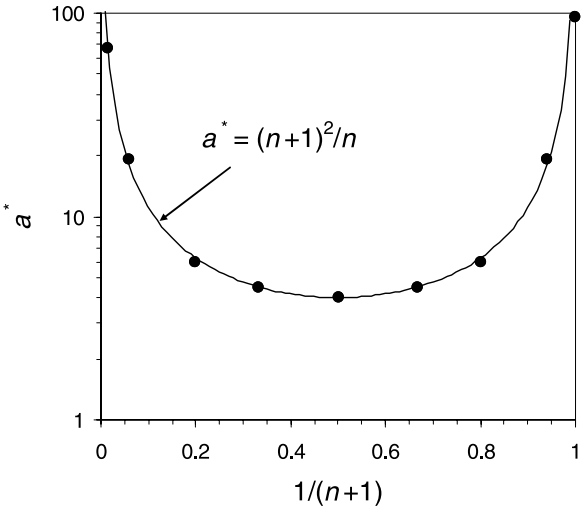

Figure 14. Dimensionless recession parameter a^* versus $1/(n + 1)$ as determined from numerical solutions to the nonlinear Boussinesq equation with a saturated hydraulic conductivity that increases as a power of n with height z above the impermeable base.

against $1/(n + 1)$. Curve fitting by trial and error to the points in Figure 14 led to

$$a^* = y^{-1}(1 - y)^{-1}, \tag{34}$$

where $y = 1/(n + 1)$, or simply $a^* = (n + 1)^2/n$. For very small values of n, including $n = 0$, (34) is inappropriate, so a modification could be made to (22) such as $a^* = (n + 1)^2/(n + 0.01)$. Finally, substituting (17), (18), (33), and (34) into (32) yields

$$dQ/dt = \frac{(n+1)^2}{(n+0.01)\varphi B}\left[\frac{k_D \sin\phi}{(n+1)(2LD)^n}\right]^{\frac{1}{n+1}} Q^{\frac{2n+1}{n+1}}. \tag{35}$$

Equation (35) was validated by plotting on one graph many numerically generated recession curves as dQ^*_g/dt^*_g against a^* $(Q^*_g)^b$. It is evident from the convergence of the curves in Figure 15 that (35) is a good approximation of late-time recession discharge for the range of parameters tested.

[56] It is of interest to compare the late-time result (equations (32) and (33)) to the analytical solution for drought flow derived for TOPMODEL given a power law transmissivity profile [*Ambroise et al.*, 1996; *Duan and Miller*, 1997; *Iorgulescu and Musy*, 1997]. Subsurface flow per unit contour length in TOPMODEL is assumed to be equal to the local topographic gradient tan β multiplied by the transmissivity T, which itself is a function of the soil moisture deficit δ [*Beven and Kirkby*, 1979]. Following *Duan and Miller* [1997], the subsurface flow given as function of the soil moisture deficit δ taken to a power m is

$$q = T \tan\beta = T_0(\tan\beta)(1 - \delta/m)^m, \tag{36}$$

where T_0 is the transmissivity at saturation, or at $\delta = 0$ [*Duan and Miller*, 1997]. Defining a degree of storage S, where $S = 1 - \delta/m$, equation (24) can be rewritten as

$$q = T_0(\tan\beta)S^m. \tag{37}$$

Note that (37) resembles the nonlinear reservoir discharge equation $Q = \alpha S^m$, where α is a constant of proportionality. Given in terms of the Boussinesq aquifer discussed in this paper, (37) becomes

$$q = T_D \tan\phi (h/D)^{n+1}, \tag{38}$$

where $T_D = k_D D/(n + 1)$ and $m = n + 1$. (As an aside, (38) is nearly identical to the flux term in the kinematic wave approximation [*Beven*, 1982b], except that tan ϕ has replaced sin ϕ.)

[57] When m and T_0, or similarly n and T_D, are uniformly distributed throughout a catchment, it has been shown [*Duan and Miller*, 1997; *Iorgulescu and Musy*, 1997] that the subsurface discharge to the channel under drought conditions can be expressed in the form of (2) with $b = (2m - 1)/m$. The lumped nonlinear reservoir equation also results in $b = (2m - 1)/m$ [*Brutsaert and Nieber*, 1977], which is expected as it is identical in form to (37). Expressed in terms of n, $b = (2n + 1)/(n + 1)$, which is equivalent to (33). In short, given a power law k profile, the nonlinear Boussinesq equation for a sloping aquifer

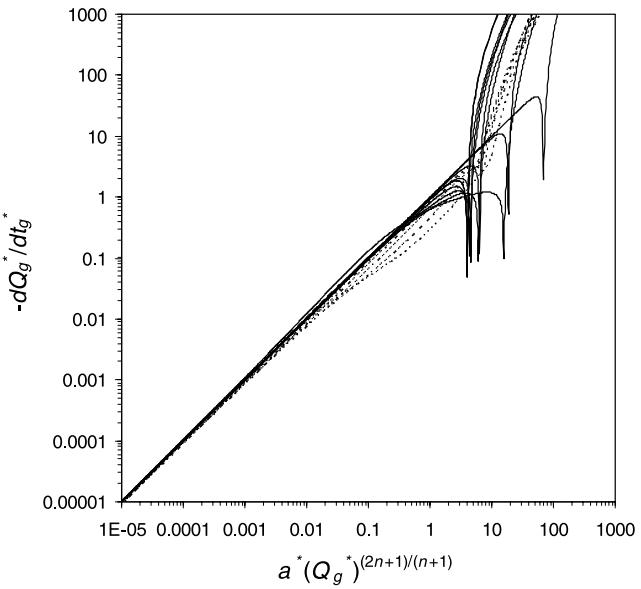

Figure 15. Dimensionless time rate of change of discharge versus transformed dimensionless discharge for various numerical solutions of the nonlinear Boussinesq equation with a saturated hydraulic conductivity that increases as a power of n with height z above the impermeable base. For all cases, the aquifer was initially saturated to a height $z = D$. The power n was varied from 0.25 to 4 for an aquifer gradient tan ϕ of 0.03 (dotted lines) and from 0.0625 to 64 for tan $\phi = 0.3$ (solid lines). For other parameter values, see Figure 3.

predicts the same value for b during late-time drought conditions as does the TOPMODEL groundwater outflow equation.

5. Conclusions

[58] This study has addressed two topics in the theory of groundwater discharge to streams from unconfined aquifers. The first topic is the effect on discharge predictions arising from the linearization methods used to derive analytical solutions to the 1-D Boussinesq equation for a sloping aquifer. Particular attention was placed on how the analytical solutions appeared when plotted as $\log(-dQ/dt)$ versus $\log(Q)$. This plotting technique has been used previously to compare recession data with analytical solutions to the Boussinesq equation for a horizontal aquifer. Known also as the method of *Brutsaert and Nieber* [1977], it is the primary analytical tool available for estimating basin-scale hydraulic properties [*Szilagyi*, 2004].

[59] It was shown by comparison with numerically generated recession curves of the nonlinear Boussinesq equation that the existing analytical solutions for the sloping aquifer are generally inappropriate for this type of analysis. An exception may be for when the water height in the stream does not differ greatly from the height of the water table relative to the total depth of the aquifer. Even in this case, however, a better theory is needed for what the effective water table height should be in the linearized equation, i.e., what is the value of pD? Given the weaknesses of the existing analytical solutions, we have presented approximate empirically obtained analytical relationships linking aquifer parameters to the discharge patterns predicted by the nonlinear Boussinesq equation.

[60] The second topic of this paper is on the use of the nonlinear 1-D Boussinesq equation for characterizing the subsurface of a hillslope with shallow soils. The Boussinesq equation in its basic form assumes a homogeneous aquifer. However, soil hydraulic properties, and particularly saturated hydraulic conductivity k, often vary with depth. We allowed lateral k to vary continuously with height h as a power law and solved the modified Boussinesq equation numerically. It was found that the recession parameter b in (2) converges to $(2n + 1)/(n + 1)$, where n is the power in the k function. A definition for the recession parameter a was also derived for late time, meaning that in theory the Brutsaert and Nieber method can be used to determine the hydraulic properties of a sloping aquifer. The findings that b can range from 1 to 2 for such a sloping aquifer and from 1.5 to 2 for the horizontal case [*Rupp and Selker*, 2005] are significant in light of streamflow recession analyses that have found values of b ranging from approximately 1 to greater than 3 [*Brutsaert and Nieber*, 1977; *Vogel and Kroll*, 1992; *Troch et al.*, 1993; *Brutsaert and Lopez*, 1998; *Szilagyi and Parlange*, 1998; *Eng and Brutsaert*, 1999; *Mendoza et al.*, 2003; *Tague and Grant*, 2004; *Malvicini et al.*, 2005]. While his analysis method differed from those in the above studies, *Wittenberg* [1999] found in effect that the distribution of b for nearly 100 streams and rivers across Germany was centered near 1.5.

[61] Though in the above work we have begun to extend the Brutsaert and Nieber method to recession discharge from individual sloping aquifers, the issue of catchment-scale applicability is still largely unexplored. The method relies on the assumption of geometric similarity of the ensemble of hillslopes that make up a catchment, while actual aquifer units will have a variety of geometries. One would expect drainage to occur faster from units that are steep, short, and/or have divergent flow lines, thereby as time progresses the hydrograph will become dominated by the aquifer units with the mildest slope, longest base, and/or most convergent flow [*Brutsaert*, 2005]. In fact, recession slope data in some sites of moderate to high relief have been found to be consistent with a nonlinear, horizontal, homogeneous Boussinesq aquifer [*Mendoza et al.*, 2003; *Tague and Grant*, 2004]. Adding to the general uncertainty on the subject is that multicatchment comparisons have not universally found slope to be an important factor in explaining drought flow variability among basins [*Zecharias and Brutsaert*, 1988a; *Vogel and Kroll*, 1992; *Lacey and Grayson*, 1998].

[62] In the case of a horizontal or very mildly sloping aquifer, *Szilagyi et al.* [1998] found the assumption of a representative single rectangular aquifer to be robust, based on numerical solutions of the 2-D Boussinesq equation in a synthetic catchment. The general shape of the recession slope curve for catchment discharge was similar to that for discharge from a 1-D rectangular aquifer, though with a smoother transition between the early and late time domains. Furthermore, the basin-scale hydraulic and geometric aquifer parameters were reasonably estimated by recession slope analysis using (2), including cases where the saturated hydraulic conductivity varied across the catchment. As of yet, however, we are not aware of numerical experiments similar to that of *Szilagyi et al.* [1998] for catchments composed of hillslopes of moderate to steep gradient.

[63] Advances have been made in applying a modified 1-D Boussinesq equation to a single hillslope with a geometry other than simply rectangular in both the planar and profile dimensions, thus allowing for divergent and convergent flow [*Paniconi et al.*, 2003; *Troch et al.*, 2003; *Hilberts et al.*, 2004; *Troch et al.*, 2004; *Huyck et al.*, 2005]. The analytical solutions derived so far, however, are still based on linearizing the modified Boussinesq equation [*Troch et al.*, 2004; *Huyck et al.*, 2005], and thus attempts at aquifer characterization using these analytical solutions [e.g., *Huyck et al.*, 2005] will still suffer from the inability of the linearized equation to accurately reproduce the correct relationship between the hydrograph slope and the discharge.

Appendix A

[64] Figure 2 lists the functions f_{Lo}, f_{R1}, and f_{R2} that are part of the definitions for the recession parameter a for three solutions to the Boussinesq equation for a horizontal aquifer. The definitions of these three functions are given below.

[65] For the early-time solution with a nonzero head h_0 in the channel, f_{Lo} is a rather complex function of h_0 and D [*Lockington*, 1997]. However, f_{Lo} takes on a narrow range of values between 1.136 and 0.785 and can be approximated by a polynomial function. The following

third-order polynomial can be used for f_{Lo} with little loss in accuracy:

$$f_{Lo} = -0.4604(h_0/D)^3 + 1.0734(h_0/D)^2 - 0.9673(h_0/D) + 1.1361. \quad \text{(A1)}$$

[66] For the early-time solution given the power law saturated hydraulic conductivity profile in (5), f_{R1} is [*Rupp and Selker*, 2005]

$$f_{R1} = \frac{(1-\mu)(n+1)(n+2)}{2(1-2\mu)}, \quad \text{(A2)}$$

where

$$\mu = \frac{4 - 3\gamma - \sqrt{\gamma^2 - 2\gamma + 4}}{4(1-2\gamma)} \quad \text{(A3)}$$

$$\gamma = 2(n+2)\mathrm{B}_{R1}. \quad \text{(A4)}$$

The parameter B_{R1} is the beta function evaluated at $n + 2$ and 2, i.e., B(n + 2, 2), or

$$\mathrm{B}_{R1} = \int_0^1 v^{n+1}(1-v)dv, \quad \text{(A5)}$$

where ν is a dummy variable of integration.

[67] For the late-time solution given the power law saturated hydraulic conductivity profile in (5), f_{R2} is [*Rupp and Selker*, 2005]

$$f_{R2} = (n+2)\left[\frac{\mathrm{B}_{R2}}{(n+3)}\right]^{\frac{1}{n+2}}, \quad \text{(A6)}$$

where B_{R2} is the beta function evaluated at $(n + 2)/(n + 3)$ and 1/2:

$$\mathrm{B}_{R2} = \int_0^1 v^{-1/(n+3)}(1-v)^{-1/2}dv. \quad \text{(A7)}$$

[68] **Acknowledgments.** This work was supported in part by National Science Foundation grant INT-0203787 and the Oregon Experiment Station. The authors thank Jan Boll for input on an early draft of this paper, and Wilfried Brutsaert and two anonymous reviewers for their constructive comments.

References

Ambroise, B., K. Beven, and J. Freer (1996), Toward a generalization of the TOPMODEL concepts: Topographic indices of hydrological similarity, *Water Resour. Res.*, *32*, 2135–2145.

Beven, K. (1981), Kinematic subsurface stormflow, *Water Resour. Res.*, *17*, 1419–1424.

Beven, K. (1982a), On subsurface stormflow: An analysis of response times, *Hydrol. Sci. J.*, *27*, 505–521.

Beven, K. (1982b), On subsurface stormflow: Predictions with simple kinematic theory for saturated and unsaturated flows, *Water Resour. Res.*, *18*, 1627–1633.

Beven, K. (1984), Infiltration into a class of vertically non-uniform soils, *Hydrol. Sci. J.*, *29*, 425–434.

Beven, K., and M. J. Kirkby (1979), A physically-based variable contributing-area model of catchment hydrology, *Hydrol. Sci. Bull.*, *24*, 43–69.

Bonell, M., D. A. Gilmour, and D. F. Sinclair (1981), Soil hydraulic properties and their effect on surface and subsurface water transfer in a tropical rainforest catchment, *Hydrol. Sci. Bull.*, *26*, 1–18.

Boussinesq, J. (1877), Essai sur la théorie des eaux courantes, *Mem. Acad. Sci. Inst. Fr.*, *23*, 252–260.

Boussinesq, J. (1903), Sur le débit, en temps de sécheresse, d'une source alimentée par une nappe d'eaux d'infiltration, *C. R. Hebd. Seanc. Acad. Sci. Paris*, *136*, 1511–1517.

Boussinesq, J. (1904), Recherches théoriques sur l'écoulement des nappes d'eau infiltrées dans le sol et sur débit de sources, *J. Math. Pures Appl.*, *10*, 5–78.

Brooks, E. S., J. Boll, and P. A. McDaniel (2004), A hillslope-scale experiment to measure lateral saturated hydraulic conductivity, *Water Resour. Res.*, *40*, W04208, doi:10.1029/2003WR002858.

Brutsaert, W. (1994), The unit response of groundwater outflow from a hillslope, *Water Resour. Res.*, *30*, 2759–2763.

Brutsaert, W. (2005), *Hydrology: An Introduction*, Cambridge Univ. Press, New York.

Brutsaert, W., and J. P. Lopez (1998), Basin-scale geohydrologic drought flow features of riparian aquifers in the southern Great Plains, *Water Resour. Res.*, *34*, 233–240.

Brutsaert, W., and J. L. Nieber (1977), Regionalized drought flow hydrographs from a mature glaciated plateau, *Water Resour. Res.*, *13*, 637–643.

Chapman, T. (1995), Comment on "The unit response of groundwater outflow from a hillslope" by Wilfried Brutsaert, *Water Resour. Res.*, *31*, 2377–2378.

Childs, E. C. (1971), Drainage of groundwater resting on a sloping bed, *Water Resour. Res.*, *7*, 1256–1263.

Duan, J., and N. L. Miller (1997), A generalized power function for the subsurface transmissivity profile in TOPMODEL, *Water Resour. Res.*, *33*, 2559–2562.

Eng, K., and W. Brutsaert (1999), Generality of drought flow characteristics within the Arkansas River basin, *J. Geophys. Res.*, *104*, 19,435–19,441.

Hall, F. R. (1968), Base-flow recessions: A review, *Water Resour. Res.*, *4*, 973–983.

Hammad, H. Y., R. Carravetta, and J. Y. Ding (1966), Discussions of "Inflow hydrographs from large unconfined aquifers", *J. Irrig. Drain. Div. Am. Soc. Civ. Eng.*, *92*, 101–107.

Harr, R. D. (1977), Water flux in soil and subsoil on a steep forested hillslope, *J. Hydrol.*, *33*, 37–58.

Henderson, F. M., and R. A. Wooding (1964), Overland flow and groundwater flow from a steady rainfall of finite duration, *J. Geophys. Res.*, *69*, 1531–1540.

Hilberts, A. G. J., C. Paniconi, E. E. Van Loon, and P. A. Troch (2004), The hillslope-storage Boussinesq model for non-constant bedrock slope, *J. Hydrol.*, *291*, 160–173.

Huyck, A. A. O., V. R. N. Pauwels, and N. E. C. Verhoest (2005), A base flow separation algorithm based on the linearized Boussinesq equation for complex hillslopes, *Water Resour. Res.*, *41*, W08415, doi:10.1029/2004WR003789.

Ibrahim, H. A., and W. Brutsaert (1965), Inflow hydrographs from large unconfined aquifers, *J. Irrig. Drain. Div. Am. Soc. Civ. Eng.*, *91*, 21–38.

Ibrahim, H. A., and W. Brutsaert (1966), Closure to "Inflow hydrographs from large unconfined aquifers", *J. Irrig. Drain. Div. Am. Soc. Civ. Eng.*, *92*, 68–69.

Iorgulescu, I., and A. Musy (1997), A generalization of TOPMODEL for a power law transmissivity profile, *Hydrol. Processes*, *11*, 1353–1355.

Koussis, A. D. (1992), A linear conceptual subsurface storm flow model, *Water Resour. Res.*, *28*, 1047–1052.

Lacey, G. C., and R. B. Grayson (1998), Relating baseflow to catchment properties in south-eastern Australia, *J. Hydrol.*, *204*, 231–250.

Lockington, D. A. (1997), Response of unconfined aquifer to sudden change in boundary head, *J. Irrig. Drain. Div. Am. Soc. Civ. Eng.*, *123*, 24–27.

Malvicini, C. F., T. S. Steenhuis, M. T. Walter, J.-Y. Parlange, and M. F. Walter (2005), Evaluation of spring flow in the uplands of Matalom, Leyte, Philippines, *Adv. Water Resour.*, *28*, 1083–1090.

Mendoza, G. F., T. S. Steenhuis, M. T. Walter, and J. Y. Parlange (2003), Estimating basin-wide hydraulic parameters of a semi-arid mountainous watershed by recession-flow analysis, *J. Hydrol.*, *279*, 57–69.

Mizumura, K. (2002), Drought flow from hillslope, *J. Hydrol. Eng.*, *7*, 109–115.

Mizumura, K. (2005), Recession analysis of drought flow using Hele Shaw model, *J. Hydrol. Eng.*, *10*, 125–132.

Paniconi, C., P. A. Troch, E. E. Van Loon, and A. G. J. Hilberts (2003), Hillslope-storage Boussinesq model for subsurface flow and variable source areas along complex hillslopes: 2. Intercomparison with a three-dimensional Richards equation model, *Water Resour. Res.*, *39*(11), 1317, doi:10.1029/2002WR001730.

Parlange, J.-Y., F. Stagnitti, A. Heilig, J. Szilagyi, M. B. Parlange, T. S. Steenhuis, W. L. Hogarth, D. A. Barry, and L. Li (2001), Sudden drawdown and drainage of a horizontal aquifer, *Water Resour. Res.*, *37*, 2097–2101.

Pauwels, V. R. N., N. E. C. Verhoest, and F. P. De Troch (2002), A meta-hillslope model based on an analytical solution to a linearized Boussinesq equation for temporally variable recharge rates, *Water Resour. Res.*, *38*(12), 1297, doi:10.1029/2001WR000714.

Pauwels, V. R. N., N. E. C. Verhoest, and F. P. De Troch (2003), Water table profiles and discharges for an inclined ditch-drained aquifer under temporally variable discharge, *J. Irrig. Drain. Div. Am. Soc. Civ. Eng.*, *129*, 93–99.

Polubarinova-Kochina, P. Y. (1962), *Theory of Ground Water Movement*, 613 pp., Princeton Univ. Press, Princeton, N. J.

Rupp, D. E., and J. S. Selker (2005), Drainage of a horizontal Boussinesq aquifer with a power law hydraulic conductivity profile, *Water Resour. Res.*, *41*, W11422, doi:10.1029/2005WR004241.

Rupp, D. E., and J. S. Selker (2006), Information, artifacts, and noise in dQ/dt-Q recession analysis, *Adv. Water Resour.*, *29*, 154–160.

Rupp, D. E., J. M. Owens, K. L. Warren, and J. S. Selker (2004), Analytical methods for estimating saturated hydraulic conductivity in a tile-drained field, *J. Hydrol.*, *289*, 111–127.

Sanford, W. E., J. Y. Parlange, and T. S. Steenhuis (1993), Hillslope drainage with sudden drawdown: Closed form solution and laboratory experiments, *Water Resour. Res.*, *29*, 2313–2321.

Stagnitti, F., L. Li, J.-Y. Parlange, W. Brutsaert, D. A. Lockington, T. S. Steenhuis, M. B. Parlange, D. A. Barry, and W. L. Hogarth (2004), Drying front in a sloping aquifer: Nonlinear effects, *Water Resour. Res.*, *40*, W04601, doi:10.1029/2003WR002255.

Steenhuis, T. S., F. Stagnitti, M. F. Walter, J. Y. Parlange, W. E. Sanford, and A. Heilig (1999), Can we distinguish Richards' and Boussinesq's equations for hillslopes? The Coweeta experiment revisited, *Water Resour. Res.*, *35*, 589–595.

Szilagyi, J. (2004), Vadose zone influences on aquifer parameter estimates of saturated-zone hydraulic theory, *J. Hydrol.*, *286*, 78–86.

Szilagyi, J., and M. B. Parlange (1998), Baseflow separation based on analytical solutions of the Boussinesq equation, *J. Hydrol.*, *204*, 251–260.

Szilagyi, J., M. B. Parlange, and J. D. Albertson (1998), Recession flow analysis for aquifer parameter determination, *Water Resour. Res.*, *34*, 1851–1857.

Tague, C., and G. Grant (2004), A geological framework for interpreting the low-flow regimes of Cascade streams, Willamette River Basin, Oregon, *Water Resour. Res.*, *40*, W04303, doi:10.1029/2003WR002629.

Tallaksen, L. M. (1995), A review of baseflow recession analysis, *J. Hydrol.*, *165*, 349–370.

Troch, P. A., F. P. De Troch, and W. Brutsaert (1993), Effective water table depth to describe initial conditions prior to storm rainfall in humid regions, *Water Resour. Res.*, *29*, 427–434.

Troch, P. A., C. Paniconi, and E. E. Van Loon (2003), Hillslope-storage Boussinesq model for subsurface flow and variable source areas along complex hillslopes: 1. Formulation and characteristic response, *Water Resour. Res.*, *39*(11), 1316, doi:10.1029/2002WR001728.

Troch, P. A., A. H. Van Loon, and A. G. J. Hilberts (2004), Analytical solution of the linearized hillslope-storage Boussinesq equation for exponential hillslope width functions, *Water Resour. Res.*, *40*, W08601, doi:10.1029/2003WR002850.

van de Giesen, N. C., T. S. Steenhuis, and J.-Y. Parlange (2005), Short- and long-time behavior of aquifer dainage after slow and sudden recharge according to the linearized Laplace equation, *Adv. Water Resour.*, *28*, 1122–1132.

Verhoest, N. E. C., and P. A. Troch (2000), Some analytical solutions of the linearized Boussinesq equation with recharge for a sloping aquifer, *Water Resour. Res.*, *36*, 793–800.

Verhoest, N. E. C., V. R. N. Pauwels, P. A. Troch, and F. P. De Troch (2002), Analytical solution for transient water table heights and outflows from inclined ditch-drained terrains, *J. Irrig. Drain. Div. Am. Soc. Civ. Eng.*, *128*, 358–364.

Vogel, R. M., and C. N. Kroll (1992), Regional geohydrologic-geomorphic relationships for the estimation of low-flow statistics, *Water Resour. Res.*, *28*, 2451–2458.

Wittenberg, H. (1999), Baseflow recession and recharge as nonlinear storage processes, *Hydrol. Processes*, *13*, 715–726.

Zecharias, Y. B., and W. Brutsaert (1988a), The influence of basin morphology on groundwater outflow, *Water Resour. Res.*, *24*, 1645–1650.

Zecharias, Y. B., and W. Brutsaert (1988b), Recession characteristics of groundwater outflow and base flow from mountainous watersheds, *Water Resour. Res.*, *24*, 1651–1658.

D. E. Rupp, National Institute of Water and Atmospheric Research, P.O. Box 8602, Christchurch 8004, New Zealand. (d.rupp@niwa.co.nz)

J. S. Selker, Department of Biological and Ecological Engineering, Oregon State University, 116 Gilmore Hall, Corvallis, OR 97331-3906, USA. (selkerj@engr.orst.edu)